

La doping effects on intergrowth Bi_2WO_6 – $\text{Bi}_3\text{TiNbO}_9$ ferroelectrics

Z.G. Yi, Y.X. Li*, Q.B. Yang, Q.R. Yin

State Key Laboratory of High Performance Ceramics and Superfine Microstructures, Shanghai Institute of Ceramics,
Chinese Academy of Sciences, 1295 Dingxi Road, Shanghai 200050, PR China

Available online 25 September 2007

Abstract

La doping effects on intergrowth Bi_2WO_6 – $\text{Bi}_3\text{TiNbO}_9$ ferroelectric ceramics were studied by X-ray diffraction, electron probe microanalysis and dielectric spectroscopy. It was found that the La^{3+} distribution, ferroelectric phase transition and dielectric relaxation behavior are apparently affected by La doping. With increasing La^{3+} content, the site of dopant ion varies, the grain growth of $\text{Bi}_5\text{TiNbWO}_{15}$ is restrained, the Curie temperature is reduced and broadened. Furthermore, two dielectric relaxation loss peaks were observed both in temperature and frequency spectra. The calculated relaxation parameters revealed the oxygen vacancy related to the relaxation process.

© 2007 Elsevier Ltd and Techna Group S.r.l. All rights reserved.

Keywords: C. Dielectric properties; C. Impedance; C. Ferroelectric properties

1. Introduction

Ferroelectric materials and their devices are very hotly pursued fields for their potential applications in information technology. It is of great importance to develop materials with a large remanent polarization P_r , low coercive field E_c , good fatigue resistance, etc. Many of previous studies have focused on $\text{Pb}(\text{Ti}, \text{Zr})\text{O}_3$ (PZT), but its inferior fatigue properties with platinum electrodes and the toxicity of lead restrict severely its applications [1]. Recently, the environmental friendly intergrowth bismuth layer-structured ferroelectrics (IBLSFs), discovered by Kikuchi et al. [2], have received a renewed interest as a promising candidate for device applications with a relatively large remanent polarization (P_r) [3], and thus open up a new avenue to enhance the dielectric and ferroelectric properties. This kind of materials can be described as a regular intergrowth of usual BLSFs along c -axis, with the difference of the numbers of perovskite-like layers that sandwiched between $(\text{Bi}_2\text{O}_2)^{2+}$ layers equals unity ($m - n = 1$). For example, the intergrowth BLSFs, $\text{Bi}_5\text{TiNbWO}_{15}$, is made up of $\text{Bi}_3\text{TiNbO}_9$ ($m = 2$) and Bi_2WO_6 ($n = 1$) along the c -axis. To this kind of natural superlattice structure, the origin of enhanced spontaneous polarization and dielectric anomalies have also

stimulated increasing attention both from a fundamental perspective and from a novel applications viewpoint [4–6]. The structure–property optimization has been carried out for $\text{SrBi}_8\text{Ti}_7\text{O}_{27}$ through La^{3+} , Sm^{3+} , and Nd^{3+} substitution for Bi^{3+} [6]. It is found that La doping has great influence on the dielectric and ferroelectric properties. In the present paper, $\text{Bi}_5\text{TiNbWO}_{15}$ ceramics are modified by La^{3+} substitution for Bi^{3+} , and the lattice constants, Curie temperature, dielectric relaxation behavior and mechanisms are investigated.

2. Experimental procedure

$\text{Bi}_{5-x}\text{La}_x\text{TiNbWO}_{15}$ ceramics ($x = 0, 0.25, 0.50, 0.75, 1.00, 1.25$ and 1.50) were synthesized by a solid-state reaction process from high pure Bi_2O_3 (99%), TiO_2 (99%), La_2O_3 (99.99%), Nb_2O_5 (99.5%), and WO_3 (99%) raw powders. The details of sample preparation can be seen in our previous paper [7]. The dielectric characteristics were measured by the impedance spectra of Pt-pasted samples using an HP4194A impedance analyzer in air at a heating rate of 3 K/min.

3. Results and discussion

The crystal structure of $\text{Bi}_5\text{TiNbWO}_{15}$ can be described as a regular intergrowth of the ‘component’ Aurivillius phases Bi_2WO_6 and $\text{Bi}_3\text{TiNbO}_9$, with the space group $Ima2$ and the lattice constants a , b and c equal to 4.1744, 0.54027 and

* Corresponding author. Tel.: +86 21 52411066; fax: +86 21 52413122.

E-mail address: yxli@mail.sic.ac.cn (Y.X. Li).

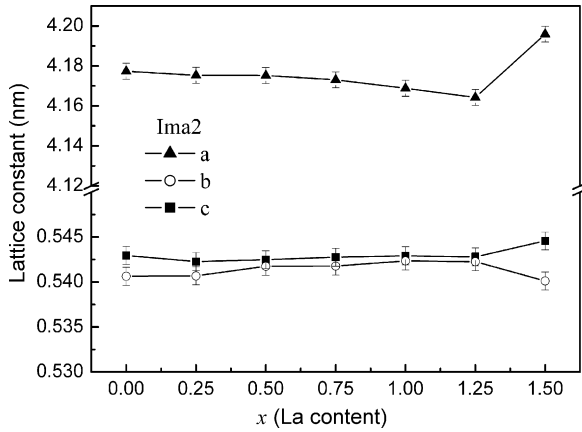


Fig. 1. Variation of lattice constants of $\text{Bi}_{5-x}\text{La}_x\text{TiNbWO}_{15}$ samples as a function of La content x .

0.54231 nm, respectively [4]. The XRD patterns (not shown) of $\text{Bi}_{5-x}\text{La}_x\text{TiNbWO}_{15}$ powders presented mono-phase crystal with the same structure and no second phase was detected. The coincidence of diffraction peaks for the samples at various x values indicates that La^{3+} doping does not affect the crystal structure. Fig. 1 shows the refined lattice constants estimated by the Rietveld method. With increasing La^{3+} doping content, there are two relatively apparent transitions occurred at $x = 0.50$ and 1.25. It is widely accepted that, $(\text{Bi}_2\text{O}_2)^{2+}$ is a rigid layer and when substituting La^{3+} for Bi^{3+} , La^{3+} will preferentially enter A sites of perovskite-like (ABO_3) layers [8]. However, when $x > 1.00$ for the compounds $\text{Bi}_{5-x}\text{La}_x\text{TiNbWO}_{15}$, the La^{3+} will definitely enter into $(\text{Bi}_2\text{O}_2)^{2+}$ layers. So the lattice constants transition at $x = 0.50$ implies the position variations for the substituting La^{3+} , i.e., when $x \geq 0.75$, the Bi^{3+} in $(\text{Bi}_2\text{O}_2)^{2+}$ begins to be substituted. This suggestion is supported by the dielectric spectroscopy and Raman spectroscopy experiments [9]. While the lattice constants transition at $x = 1.25$ reveals that too much La^{3+} substitution in the rigid $(\text{Bi}_2\text{O}_2)^{2+}$ layers will deteriorate the bismuth layered perovskite structure. In fact, a secondary phase was observed when La^{3+} content was above 1.50.

Fig. 2 shows the temperature dependence of dielectric permittivity and dielectric loss of intergrowth BLSFs $\text{Bi}_{5-x}\text{La}_x\text{TiNbWO}_{15}$ at a frequency of 1 MHz. For the La^{3+} un-doped sample, a dielectric anomaly peak is observed at ~ 1100 K. With increasing La^{3+} doping content, the dielectric anomaly peak shifts to a lower temperature range and, when $x \geq 0.75$, it becomes broad and diffusive. From these phenomena, it can be concluded that the phase transition temperature, T_c , shifts to lower temperature range with increasing La doping content. The decrease of T_c is due to the substitution of La^{3+} for Bi^{3+} , as the $6s^2$ lone pair electrons of Bi^{3+} have great influence on the Curie temperature [10]. The diffusive character of phase transition peak occurred at $x \geq 0.75$ implies that there is site disorder in $\text{Bi}_{5-x}\text{La}_x\text{TiNbWO}_{15}$ ceramics ($x = 0.75, 1.00, 1.25$ and 1.50). It is apparent from the relative b/c cell dimensions reported for Bi_2WO_6 (0.5458 and 0.5437 nm), $\text{Bi}_3\text{TiNbO}_9$ (0.5440 and 0.5394 nm), and $\text{Bi}_5\text{TiNbWO}_{15}$ (0.5423 and 0.5403 nm) [4,11] that the perovskite-like layer [WO_4] is under

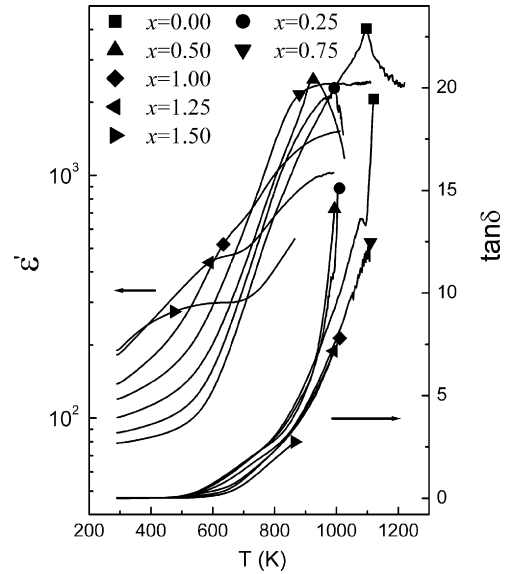


Fig. 2. The dielectric permittivity and dielectric loss of $\text{Bi}_{5-x}\text{La}_x\text{TiNbWO}_{15}$ ceramics as a function of temperature, measured at 1 MHz.

compressive stress compared to the perovskite-like layers [BiTiNbO_7]. Furthermore, from the variations of lattice constants of $\text{Bi}_{5-x}\text{La}_x\text{TiNbWO}_{15}$, it can be seen that the stress is aggravated by A-site substitution. The sites disorder occurred at $x \geq 0.75$ helps relaxing the lattice mismatch and is consistent with the viewpoint mentioned above that Bi^{3+} in $(\text{Bi}_2\text{O}_2)^{2+}$ layers begins to be substituted at $x = 0.75$. Additionally, from Fig. 2, it can be observed that the dielectric loss increases rapidly with increasing temperature. Fortunately, the substituting La^{3+} for Bi^{3+} in $(\text{Bi}_2\text{O}_2)^{2+}$ can reduce dramatically the dielectric loss at high temperatures.

Fig. 3 shows the dielectric loss ($\tan \delta$) and dielectric permittivity of the $\text{Bi}_5\text{TiNbWO}_{15}$ specimen as a function of temperature measured at three different frequencies (0.1, 1 and 10 kHz). Two apparent dielectric loss peaks superimposed on a temperature-dependent background are observed at about 453 and 652 K when the frequency is 0.1 kHz and shift to higher temperature with increasing frequency. Correspondingly, there are two steps in the curves of dielectric permittivity versus

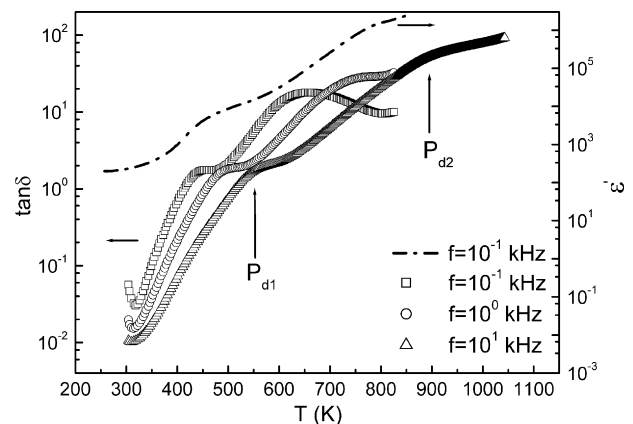


Fig. 3. Temperature dependence of the dielectric permittivity and dielectric loss of $\text{Bi}_5\text{TiNbWO}_{15}$ ceramic measured at different frequencies.

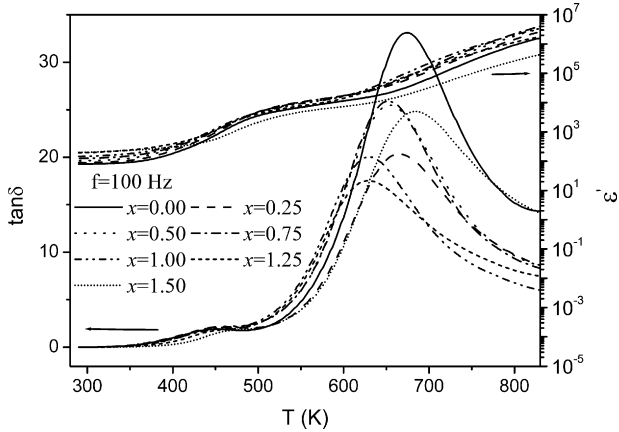


Fig. 4. Temperature dependence of the dielectric permittivity and dielectric loss of intergrowth $\text{Bi}_{5-x}\text{La}_x\text{TiNbWO}_{15}$ ferroelectrics measured at a frequency of 100 Hz.

temperature. These phenomena indicate that the two loss peaks (P_{d1} peak at lower temperature and P_{d2} peak at higher temperature) are of relaxation characteristic and associated with thermally activated relaxation process.

Fig. 4 shows the dielectric loss ($\tan \delta$) and dielectric permittivity of $\text{Bi}_{5-x}\text{La}_x\text{TiNbWO}_{15}$ specimens as a function of temperature measured at a frequency of 0.1 kHz. Similarly, two dielectric loss peaks and two dielectric permittivity steps are also observed for all the samples though there are variations in peak height and temperature.

To indicate the distinctions between these relaxation loss peaks further, Fig. 5 shows the dielectric loss ($\tan \delta$) of $\text{Bi}_{5-x}\text{La}_x\text{TiNbWO}_{15}$ specimens as a function of frequency measured at temperatures 513 and 673 K. Due to the apparent

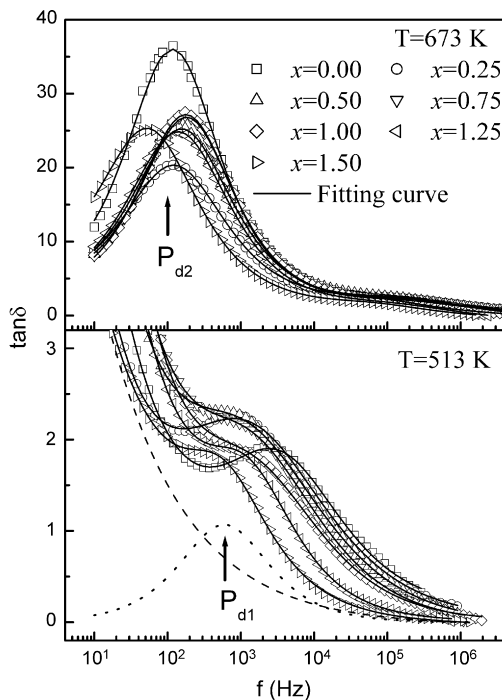


Fig. 5. Frequency dependence of the dielectric loss of $\text{Bi}_{5-x}\text{La}_x\text{TiNbWO}_{15}$ ceramics measured at temperature 513 and 673 K.

separation of the two loss peaks, it is convenient to detect the distinctions between the loss peaks of different specimens.

According to the modified Debye equation [12], the dielectric loss peak can be deduced as follows:

$$\tan \delta = \frac{2\Delta \sin(\beta\pi/2)}{\cosh(\beta z) + \cos(\beta\pi/2)}, \quad (1)$$

where Δ is the relaxation strength, $z = \ln(\omega\tau)$, $\beta = 1 - \alpha$, and α ($0 \leq \alpha < 1$) is the width parameter leading to a symmetric broadening of the Debye relaxation ($\alpha = 0$ corresponds to the standard Debye relaxation). The fitting result of frequency spectra for a specimen ($x = 1.50$) measured at 513 K is also shown in Fig. 5. It can be seen that Eq. (1) and a frequency dependent background could fit the dielectric loss curve very well, where the width parameter $\beta = 0.86$, or $\alpha = 0.14$. Here the background loss (D_{bg}), mainly comes from the static conduction of the grain, is proportional to the ratio of static conductivity (σ) over frequency (f), i.e.

$$D_{bg} \propto \frac{\sigma}{f} = \sigma_0 \exp\left(\frac{-E_{cond}/K_B T}{f}\right), \quad (2)$$

where σ_0 is the pre-exponential term and E_{cond} is the activation energy of the conductivity. Therefore, the background loss is also thermally activated and shifts toward higher frequency with increasing temperature [13]. The fit parameters for the dielectric loss ($\tan \delta$) curves of $\text{Bi}_{5-x}\text{La}_x\text{TiNbWO}_{15}$ specimens in Fig. 5 are summarized in Table 1. The variation of α values indicates that La^{3+} doping has a moderate influence on the relaxation time distribution of P_{d2} peak but it has a great effect on the relaxation time distribution of P_{d1} peak. The relaxation time distribution of P_{d1} peak broadens first, and then becomes narrower with increasing La^{3+} doping content.

For a thermally activated relaxation process, the relaxation time generally follows the Arrhenius law:

$$\tau = \tau_0 \exp\left(\frac{E}{K_B T}\right), \quad (3)$$

where τ_0 is the pre-exponential factor (or the relaxation time at infinite temperature), E denotes the activation energy of the

Table 1

Parameters obtained with the modified Debye fitting method for frequency dependence of the dielectric loss of $\text{Bi}_{5-x}\text{La}_x\text{TiNbWO}_{15}$ ceramics measured at temperature 513 and 673 K

x	P_{d1} peak			P_{d2} peak		
	Δ	ω_p (s^{-1})	α	Δ	ω_p (s^{-1})	α
0.00	100.0%	21060	0.32	100%	739.44	0.16
0.25	159.7%	7939	0.43	57.2%	774.93	0.20
0.50	152.7%	7456	0.44	71.8%	988.17	0.19
0.75	121.7%	8876	0.39	71.7%	1155.39	0.16
1.00	102.7%	9534	0.38	77.0%	1124.99	0.17
1.25	64.3%	7786	0.18	74.3%	888.25	0.20
1.50	51.6%	3708	0.16	67.4%	342.07	0.18

Δ denotes relaxation strength of the dielectric loss peaks, ω is the angular frequency and the subscript p denotes values at peak position ($\omega = 2\pi f$), and α ($0 \leq \alpha < 1$) is the width parameter leading to a symmetric broadening of the Debye relaxation.

Table 2

The activation energy and pre-exponential term of the Arrhenius law for the two dielectric loss peaks in $\text{Bi}_{5-x}\text{La}_x\text{TiNbWO}_{15}$ ceramics

x	P_{d1} peak		P_{d2} peak	
	τ_0 (s)	E (eV)	τ_0 (s)	E (eV)
0.00	2.85×10^{-14}	0.94	5.60×10^{-12}	1.08
0.25	4.19×10^{-13}	0.88	7.93×10^{-11}	0.96
0.50	1.06×10^{-12}	0.84	2.40×10^{-10}	0.88
0.75	1.00×10^{-12}	0.82	2.02×10^{-10}	0.89
1.00	1.59×10^{-12}	0.79	3.30×10^{-10}	0.86
1.25	3.65×10^{-13}	0.87	8.15×10^{-10}	0.82
1.50	5.97×10^{-13}	0.88	5.80×10^{-9}	0.76

relaxation process, T is the absolute temperature, and K_B is Boltzmann constant. It is well known that at the peak position the condition $\omega_p \tau_p = 1$ is fulfilled, where $\omega = 2\pi f$ is the angular frequency of measurement and the subscript p denotes values at peak position. Therefore, if we plot the $\ln(\omega_p)$ as a function of the reciprocal of peak temperature (Arrhenius plots), a linear relation would be obtained according to Eq. (3). The relaxation parameters E and τ_0 can thus be deduced from the slope and intercept of this line, respectively. That is the so-called Arrhenius plots and thus deduced relaxation parameters are summarized in Table 2.

Our previous work [7] has demonstrated $\text{Bi}_5\text{TiNbWO}_{15}$ is a high ionic conductor and its electrical property is related closely to oxygen vacancies. Here the dielectric relaxation mechanism in $\text{Bi}_{5-x}\text{La}_x\text{TiNbWO}_{15}$ was further discussed. From Table 2, it can be seen that the values of the relaxation parameters are comparable with the values for oxygen ion diffusion in Bi_2WO_6 [14], $\text{Bi}_4\text{Ti}_3\text{O}_{12}$ [15], $\text{YBa}_2\text{Cu}_3\text{O}_{7-\delta}$ [16], etc. The consistency in activation energy suggests a mechanism of oxygen ions diffusion via vacancies for P_{d1} and P_{d2} peaks. Furthermore, the capacitance values are $\sim 10^{-10}$ and $\sim 10^{-8}$ F for P_{d1} and P_{d2} peaks respectively, which manifest that P_{d1} peak is of bulk response and P_{d2} peak is related to grain boundary since the value $\sim 10^{-10}$ F is a characteristic one for bulk ferroelectrics and the value $\sim 10^{-8}$ F reveals that the sample is well-sintered with narrow intergranular regions.

With increasing La^{3+} content, the activation energy of P_{d2} peak decreases gradually which may be related to the evolution of grain boundary structures and further experimental and theoretical studies are necessary. Fig. 6 shows the variation of activation energy and relaxation strength at 513 K of P_{d1} peak with the increase of La^{3+} content. It is apparent that they develop different trends. The activation energy decreases firstly and when $x > 1.00$, it increases again, whereas the relaxation strength increases firstly and then decreases monotonously at $x > 0.25$.

In the case of La^{3+} doping, the ionic radii of La^{3+} are similar to that of Bi^{3+} ions where the lone-pair character of Bi^{3+} is dominant, no extra oxygen vacancies are introduced after La^{3+} doping due to the same valence of Bi^{3+} and La^{3+} ions. However, the lone-pair electrons (6s) of Bi^{3+} ions occupy a volume similar to that of an O^{2-} anion and when substituting La^{3+} for Bi^{3+} , the free volume in the lattice will increase [17]. Therefore, the activation energy of P_{d1} peak decreases and the relaxation

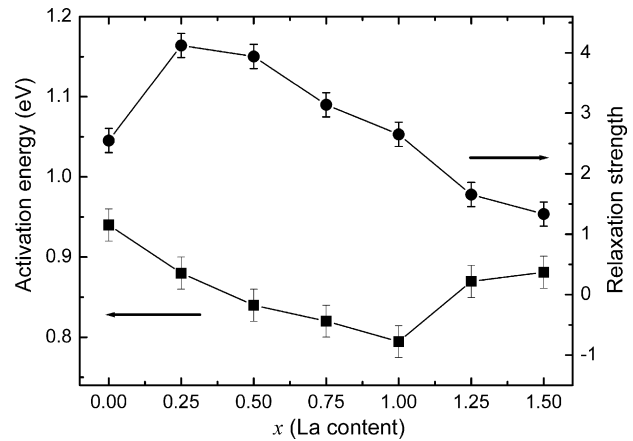


Fig. 6. Variation of the activation energy and relaxation strength of P_{d1} peak as a function of La content x .

strength of P_{d1} peak increases after La^{3+} doping. However, when an amount of La^{3+} ions are doped into the compound, the variation of activation energy and relaxation strength exhibit complexity due to the site variation of substituting La^{3+} ions, the evolution of crystal structure and the reduced volatilization of bismuth at high temperature, etc.

Moreover, Fig. 6 also reveals some details about dielectric relaxation in the compounds. It was reported in oxide ceramics, that the short-range diffusion of oxygen ions or vacancies under an oscillating electric field, similar to the reorientation of the dipole, leads to a dielectric relaxation, in which the oxygen ions or vacancies act as “polarons”. Therefore, the dielectric relaxation process of oxygen ions within the bulk materials implies information of local structure and dynamics. In our case, when the substituting La^{3+} content at $x = 0.25$ (Bi^{3+} ions at A sites of perovskite-like layers substituted), the free volume within the $[\text{BiTiNbO}_7]$ block is increased and thus favors hopping of oxygen ions coordinating A sites. At the same time, the free volume of the $[\text{WO}_4]$ block is decreased due to compressive stress compared to the $[\text{BiTiNbO}_7]$ block, thus hinders the oxygen ions diffusion within the $[\text{WO}_4]$ block. As a result, it can be inferred that P_{d1} peak is related to hopping between the coordinating oxygen ions of A sites.

4. Conclusions

Crystal structure and dielectric properties of La-doped $\text{Bi}_2\text{WO}_6\text{--Bi}_3\text{TiNbO}_9$ ferroelectrics were studied. It was found that La doping varies the sites of dopant ions, restrains the grain growth of $\text{Bi}_5\text{TiNbWO}_{15}$, reduces and broadens the Curie temperature. Furthermore, two dielectric relaxation loss peaks were observed both in temperature and frequency spectra. The calculated relaxation parameters suggest oxygen vacancy dominants the relaxation process.

Acknowledgements

This work was supported by the Ministry of Sciences and Technology of China through 973-project (No. 2002CB613307)

and 863-project (No. 2006AA03Z0430), the National Natural Science Foundation of China (No. 50572113).

References

- [1] O. Matsuura, M. Kurasawa, S. Umemiya, K. Maruyama, K. Kurihara, Influence of SRO top electrode on fatigue characteristics of FRAM, *Key Eng. Mater.* 269 (2004) 69–74.
- [2] T. Kikuchi, A. Watanabe, K. Uchida, A family of mixed-layer type bismuth compounds, *Mater. Res. Bull.* 12 (1977) 299–304.
- [3] Y. Noguchi, M. Miyayama, T. Kudo, Ferroelectric properties of intergrowth $\text{Bi}_4\text{Ti}_3\text{O}_{12}$ – $\text{SrBi}_4\text{Ti}_4\text{O}_{15}$ ceramics, *Appl. Phys. Lett.* 77 (2000) 3639–3641.
- [4] A. Snedden, D.O. Charkin, V.A. Dolgikh, P. Lightfoot, Crystal structure of the ‘mixed-layer’ Aurivillius phase $\text{Bi}_5\text{TiNbWO}_{15}$, *J. Solid State Chem.* 178 (2005) 180–184.
- [5] Y. Goshima, Y. Noguchi, M. Miyayama, Dielectric and ferroelectric anisotropy of intergrowth $\text{Bi}_4\text{Ti}_3\text{O}_{12}$ – $\text{PbBi}_4\text{Ti}_4\text{O}_{15}$ single crystals, *Appl. Phys. Lett.* 81 (2002) 2226–2228.
- [6] R.Z. Hou, X.M. Chen, S.Y. Wu, Substitution of Sm^{3+} and Nd^{3+} for Bi^{3+} in $\text{SrBi}_8\text{Ti}_7\text{O}_{27}$ mixed aurivillius phase, *Jpn. J. Appl. Phys.* 42 (2003) 5169–5171.
- [7] Z.G. Yi, Y.X. Li, Z.Y. Wen, S.R. Wang, J.T. Zeng, Q.R. Yin, Intergrowth Bi_2WO_6 – $\text{Bi}_3\text{TiNbO}_9$ ferroelectrics with high ionic conductivity, *Appl. Phys. Lett.* 86 (2005) 192906–192908.
- [8] R.E. Newnham, R.W. Wolfe, J.F. Dorrian, Structural basis of ferroelectricity in the bismuth titanate family, *Mater. Res. Bull.* 6 (1971) 1029–1039.
- [9] Z.G. Yi, Y.X. Li, J.T. Zeng, Q.B. Yang, D. Wang, Y.Q. Lu, Q.R. Yin, Lanthanum distribution and dielectric properties of intergrowth $\text{Bi}_{5-x}\text{La}_x\text{TiNbWO}_{15}$ ferroelectrics, *Appl. Phys. Lett.* 87 (2005) 202901–202903.
- [10] E.C. Subbarao, A family of ferroelectric bismuth compound, *J. Phys. Chem. Solids* 23 (1962) 665–676.
- [11] J.G. Thompson, A.D. Rae, R.L. Withers, D.C. Craig, Revised structure of $\text{Bi}_3\text{TiNbO}_9$, *Acta Crystallogr. B* 47 (1991) 174–180.
- [12] C. Ang, Z. Yu, L.E. Cross, Oxygen-vacancy-related low-frequency dielectric relaxation and electrical conduction in $\text{Bi}:\text{SrTiO}_3$, *Phys. Rev. B* 62 (2000) 228–236.
- [13] X.P. Wang, Q.F. Fang, Z.S. Li, G.G. Zhang, Z.G. Yi, Dielectric relaxation studies of Bi-doping effects on the oxygen-ion diffusion in $\text{La}_{2-x}\text{Bi}_x\text{Mo}_2\text{O}_9$ oxide-ion conductors, *Appl. Phys. Lett.* 81 (2002) 3434–3437.
- [14] N. Baux, R.N. Vannier, G. Mairesse, G. Nowogrocki, Oxide ion conductivity in $\text{Bi}_2\text{W}_{1-x}\text{ME}_x\text{O}_{6-x/2}$ ($\text{ME} = \text{Nb}, \text{Ta}$), *Solid State Ionics* 91 (1996) 243–248.
- [15] H.S. Shulman, D. Damjanovic, N. Setter, Niobium doping and dielectric anomalies in bismuth titanate, *J. Am. Ceram. Soc.* 83 (2000) 528–532.
- [16] S.J. Rothman, J.L. Roubort, J.E. Baker, Tracer diffusion of oxygen in $\text{YBa}_2\text{Cu}_3\text{O}_{7-\delta}$, *Phys. Rev. B* 40 (1989) 8852.
- [17] P. Lacorre, The LPS concept, a new way to look at anionic conductors, *Solid State Sci.* 2 (2000) 755–758.